

Thalamocortical transformations of periodic stimuli: the effect of stimulus velocity and synaptic short-term depression in the vibrissa–barrel system

Jaime de la Rocha · Néstor Parga

Received: 9 August 2005 / Revised: 26 November 2007 / Accepted: 27 November 2007 / Published online: 9 January 2008
© Springer Science + Business Media, LLC 2007

Abstract Recent works on the response of barrel neurons to periodic deflections of the rat vibrissae have shown that the stimulus velocity is encoded in the cortical spike rate (Pinto et al., *J. Neurophysiol.* 83(3): 1158–1166, 2000; Arabzadeh et al., *J. Neurosci.* 23(27): 9146–9154, 2003). Other studies have reported that repetitive pulse stimulation produces band-pass filtering of the barrel response rate centered around 7–10 Hz (Garabedian et al., *J. Neurophysiol.* 90:1379–1391, 2003) whereas sinusoidal stimulation gives an increasing rate up to 350 Hz (Arabzadeh et al., *J. Neurosci.* 23(27):9146–9154, 2003). To explore the mechanisms underlying these results we propose a simple computational model consisting in an ensemble of cells in the ventro-posterior medial thalamic nucleus (VPm) encoding the stimulus velocity in the temporal profile of their response, connected to a single barrel cell through synapses showing short-term depression. With sinusoidal stimulation, encoding the velocity in VPm facilitates the response as the stimulus frequency increases and it causes the velocity to be encoded in the cortical rate in the frequency range 20–100 Hz.

Synaptic depression does not suppress the response with sinusoidal stimulation but it produces a band-pass behavior using repetitive pulses. We also found that the passive properties of the cell membrane eventually suppress the response to sinusoidal stimulation at high frequencies, something not observed experimentally. We argue that network effects not included here must be important in sustaining the response at those frequencies.

Keywords Thalamus · Barrel · Vibrissa velocity · Short-term depression · Integrate-and-fire neuron · Firing rate · Membrane passive properties

1 Introduction

To explore their environment, rats generate motions of their whiskers moving them back and forth at frequencies in the range 4–12 Hz, a behavior called whisking (Welker 1964; Carvell and Simons 1990). A relevant issue is to determine which physical quantities associated to the whisker motion are internally used to process tactile information and how they are encoded in the whisker-to-barrel pathway. Several studies indicate that one relevant quantity is the whisker velocity. Work done using a ramp-and-hold stimulus shows that, in the ventro-posterior medial thalamic nucleus (VPm), the velocity is encoded in the temporal profile of the population response with little effect on the thalamic spike rate (ThSR), while barrel cells encode it in the cortical spike rate (CSR) (Pinto et al. 2000). Using sinusoidal stimulation, a recent work found that the CSR encodes

Action Editor: Xiao-Jing Wang

J. de la Rocha · N. Parga
Dto. de Física Teórica, Universidad Autónoma de Madrid,
28049 Madrid, Spain

J. de la Rocha (✉)
Center for Neural Science, New York University,
New York, 10003 NY, USA
e-mail: jrocha@cns.nyu.edu

some function of the product amplitude \times frequency, such as the whisker velocity itself (Arabzadeh et al. 2003).

Many works have addressed the question of whether the vibrissa–barrel system is somehow optimized to deal with specific frequency ranges (see (Moore 2004) for a review). These studies analyzed frequency ranges either around those values mimicking the whisking motion itself (1–40 Hz) (Ahissar et al. 2000; Sosnik et al. 2001; Garabedian et al. 2003) or around values similar to the resonant frequency of the whiskers (a few hundred hertz) (Arabzadeh et al. 2003; Andermann et al. 2004). However, these studies lead to apparently contradictory results: (1) experiments performed at low and moderate frequencies indicate that the CSR has a band-pass behavior, suppressing frequencies beyond 20–30 Hz (Garabedian et al. 2003) while (2) an experiment reaching high frequencies finds that it grows monotonically with the frequency (at least up to 340 Hz) (Arabzadeh et al. 2003). These differences have led some authors to hypothesize that the system has two different operating modes depending on whether the stimulation frequency is low or high (Moore 2004). However, a more fundamental understanding of the transformations taking place in the system is still lacking.

Studies in various sensory pathways have shown that thalamo-cortical (TC) short-term depression (STD; Castro-Alamancos 1997) is responsible for the suppression of the cortical response at high stimulation frequencies (Eggermont 1999; Garabedian et al. 2003). If this is the case, it would be necessary to explain the role of depression in the processing of high stimulation frequencies associated with texture coding and whether there exist stimulation conditions which avoid that suppression and lead to a high-pass filter behavior of the CSR in the presence of TC depression.

The filtering properties of individual neurons to periodic stimuli has also been the focus of analysis of many theoretical studies (Koch 1999; Hutcheon and Yarom 2000; Brunel et al. 2001; Gerstner and Kistler 2002; Svirskis and Rinzel 2003). In particular, it is well known that the passive properties of the cell membrane confer the neuron response a low pass filter behavior. However, the question of what are the limits imposed by the membrane on the ability of neurons to track very fast signals is still debated (Gerstner 2000; Brunel et al. 2001).

Here we elaborate simple and distinct models of the Vpm response to repetitive stimulation and to sinusoidal stimulation inspired on experimental data. The model includes the codification of the stimulus velocity in the temporal profile of the thalamic response and

TC connections with STD. The activity of this thalamic population will be propagated onto a single cortical recipient cell modeled as an integrate-and-fire neuron. Analyzing its cortical response we address the following questions: (1) what is the specific role of TC depression in modulating the cortical response across frequencies?; (2) can the quoted experimental studies showing velocity encoding in the CSR be reproduced and explained by simply encoding the velocity in the temporal profile of the Vpm response?

2 Methods

2.1 Stimuli

Two different stimulation paradigms will be distinguished [Fig. 1(a)]:

1. *Repetitive pulse stimulation*, which consists in the repetitive application of a pulse with a fixed shape which is independent of the frequency (e.g. air puffs or mechanical square waves). It is defined by the pulse amplitude A , the duration Σ_0 and the stimulation frequency, f [Fig. 2(a)].
2. *Sinusoidal stimulation*, characterized by the amplitude A and the frequency f of the sinusoidal wave [Fig. 5(a)].

We will first propose a model for the thalamic response to these two types of stimulus. Afterwards, we will use the thalamic responses to stimulate a single barrel cell.

2.2 Thalamic response

We consider a population of $N = 85$ thalamic cells. The response of each cell is described in terms of their cycle peri-stimulus time histogram (CPSTH), that is, the average of the steady-state peri-stimulus time histogram (PSTH) across all stimulus cycles [Fig. 1(b) right]. Experimental data obtained using short air puffs show a single peaked thalamic response, about 50 ms long, which resembles the profile of a Gamma function (Sosnik et al. 2001). Sinusoidal whisker stimulation produces a large onset peak response followed by a small offset response (Hartings et al. 2003; Khatri et al. 2004). We have neglected this small offset peak and have modeled the CPSTH in both pulse and sinusoidal stimulation with a Gamma function defined as

$$G(t) = \frac{C}{\Sigma} t e^{-t/\Sigma+1} \quad (1)$$

Σ is the time-to-peak and it also sets its temporal width, giving rise to an appreciable thalamic activity during

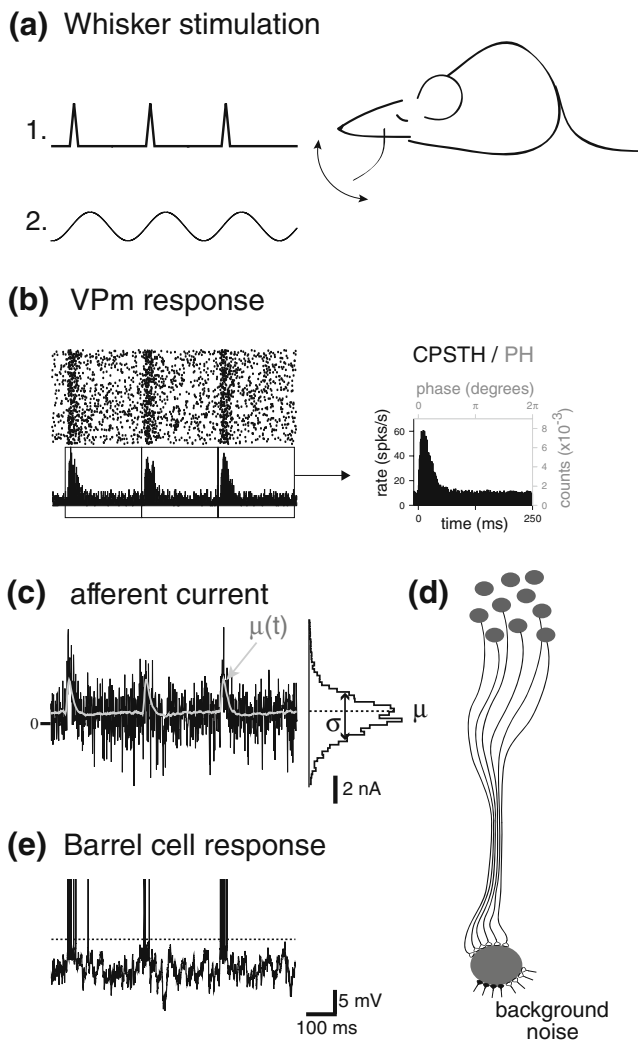


Fig. 1 Model outline. (a) The rat's whisker is deflected with a certain waveform which can be (1) a repetitive train of pulses; (2) sinusoidal stimulation (b) This produces that a population of cells in the ventro-posterior medial thalamic nucleus (VPM) increase their firing over baseline. This is modeled by generating N spike trains with the same inhomogeneous Poisson waveform whose modulation represents the encoding of the whisker deflections. The spike rastergram depicts an example of these trains with a population one-trial histogram shown below. The cycle per-stimulus time histogram (CPSTH) and the phase histogram (PH) are obtained by performing an average of the PSTH across stimulus cycles (right). (c) The spike trains from VPM go through stochastic depressing synapses to generate a stochastic afferent current with instantaneous mean $\mu(t)$ (gray), temporal mean μ and variance σ^2 (see histogram). (d) Besides the thalamocortical current component, the target cell also receives a stochastic stationary background current. (e) The model describes a barrel cell as an integrate-and-fire (LIF) model neuron, which integrates its afferent current and generates a stochastic output spike train

a time interval of about 5Σ [see inset in Fig. 2(b)]. The parameter C sets the peak response. The area under the Gamma, $e C \Sigma$, equals the mean number of action potentials (AP) per deflection discharged by a thalamic cell. Although the CPSTH in the two

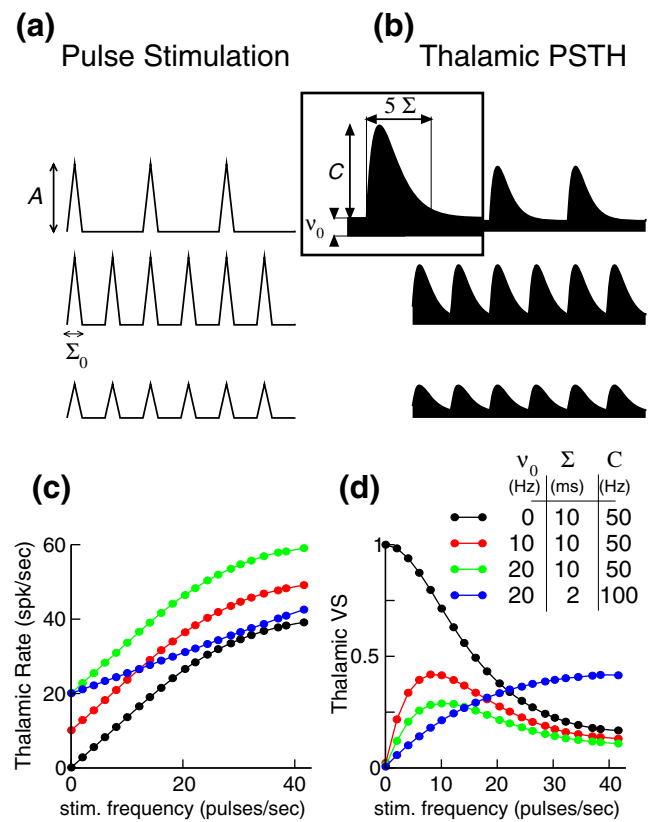


Fig. 2 Thalamic response under repetitive pulse stimulation. (a–b) Three example stimuli (a) and the corresponding PSTH's, according to our model of the VPM response (b). Each triangular pulse generates a fixed Gamma shaped response [see zoomed histogram in (b)]. An increase in frequency produces similar responses but less spaced in time. Changes in stimulation amplitude translate into changes of the peak response C with no change in the response duration. (c) The spike rate of the VPM cells increases linearly with the frequency because the number of spikes per deflection is independent of f . At high frequencies ($f > 30$ Hz) the ThSR starts to saturate because the width of the Gamma function exceeds the cycle period and it has to be truncated. (d) The VS of VPM cells can be low-pass, high-pass or band-pass depending on the values of v_0 , Σ and C (see Section 3.1.1). Parameters are as indicated in the legend

stimulation paradigms is modeled using the function $G(t)$ [Eq. (1)], the scaling of this function with the stimulation frequency will be different (see Section 3).

We define the thalamic firing with the instantaneous spike rate, $\nu(t)$, which gives the instantaneous probability of discharge of the thalamic neurons (Rieke et al. 1996). Individual spike trains are stochastic and follow an inhomogeneous Poisson process with rate $\nu(t)$. Repeated trials therefore, do not reproduce the timing of the spikes precisely, only the statistics is the same. Figure 1(b) shows the population spike rastergram from a single trial along with the population summed activity. The rate $\nu(t)$ is built from the concatenation of CPSTH's plus a basal rate, ν_0 , which represents the thalamic AP's spontaneously discharged in the absence

of stimulation (Fanselow and Nicolelis 1999; Swadlow and Gusev 2001; Castro-Alamancos and Oldford 2002; Bruno and Sakmann 2006).

$$v(t) = v_0 + \sum_k G(t - k/f) , \tag{2}$$

where each Gamma function in the sum is defined only within its corresponding stimulation period.

The mean thalamic spike rate, ThSR, can be easily computed recalling that each deflection produces an average of $eC\Sigma$ spikes. Thus, we have that

$$ThSR \simeq v_0 + eC\Sigma f . \tag{3}$$

This equality is not always exact because the duration of a deflection response, 5Σ , can become comparable to the period of the stimulation so that the Gamma has to be truncated. This clipping effect is noticeable at high frequencies in Fig. 2(c) and at low frequencies in Fig. 7(d).

2.3 Short-term depression model

The TC synapses in our model show short-term depression (STD) (Magleby 1987; Zucker and Regehr 2002; Gil et al. 1999). We use a simple model of vesicle turnover (Vere-Jones 1966; Wang 1999; de la Rocha et al. 2002), with synapses consisting of $M = 7$ functional contacts (Gil et al. 1999), each of them containing a vesicle releasable pool which can host at most one vesicle ready for release (Matveev and Wang 2000; de la Rocha and Parga 2005). When this pool is empty, spikes arriving to the terminal fail to transmit any signal. If the pool is not empty, pre-synaptic spikes can release the neurotransmitter of the releasable vesicle with probability $U = 0.8$ (Gil et al. 1999). The recovery time, i.e. the time it takes to replenish the pool with a new vesicle after a release, is random with exponential distribution and mean¹ $\tau_v = 300$ ms.

The *instantaneous transmission probability*, $P_t(t)$, quantifies the level of depression of the synapses during the stimulation. It is obtained by computing over many trials the fraction of functional contacts that, being hit by an AP at time t , elicited a synaptic response. The average probability P_t , hereafter referred to as the

transmission probability, equals the overall fraction of successful spikes.

2.4 Synaptic current

Each pre-synaptic spike can produce at most the release of M vesicles, one at each of the M contacts. The synaptic current generated by the release of a single vesicle is modeled as an instantaneous pulse of current $J \delta(t - t^k)$, being J the amplitude of the pulse and $\delta(t - t^k)$ the Dirac delta function. Thus, a train of thalamic AP's gives rise to a sequence of current pulses described as

$$I_{stim}(t) = \sum_i^N \sum_m^M J_{i,m} \sum_k^{rel} \delta(t - t_{i,m}^k) . \tag{4}$$

The sums run over thalamic neurons ($i = 1 \dots N$), over synaptic contacts ($m = 1 \dots M$), and over the releases produced at each contact ($k = 1, \dots, rel$). The efficacies $J_{i,n}$ are randomly distributed with a Gaussian of mean J and coefficient of variation $\Delta = 0.2 - 0.4$ (Gil et al. 1999). We will specify the value of the ratio J/C_m which measures the quantal amplitude in voltage units. In addition to the current generated by the thalamic spikes, we include a background current, $I_{bg}(t)$, representing the stationary activity coming from other cortical neurons [Fig. 1(d)]. $I_{bg}(t)$ is composed of an excitatory and an inhibitory Poisson trains at constant rates v_E and v_I , respectively, representing the superposition of hundreds of pre-synaptic trains at low cortical spontaneous frequencies. The background synapses are modeled as unreliable but non-depressing. The total synaptic current received by the cortical neuron is denoted as $I(t) = I_{stim}(t) + I_{bg}(t)$. Figure 1(c) illustrates a typical example of the current generated in one trial. It will be statistically described by its instantaneous mean $\mu(t)$, its temporal average μ and its temporal variance σ^2 [see Fig. 1(c) overlapped gray trace and histogram]. They are defined as

$$\mu(t) \equiv \langle I(t) \rangle \propto v(t) P_t(t) \tag{5}$$

$$\mu \equiv \frac{1}{T} \int_0^T I(t) dt \propto (ThSR) P_t \tag{6}$$

$$\sigma^2 \equiv \frac{1}{T} \int_0^T I^2(t) dt - \mu^2 . \tag{7}$$

The angular brackets denote an average over trials. Equation (5) expresses that $\mu(t)$ is proportional to the thalamic signal $v(t)$ weighted by the instantaneous transmission probability $P_t(t)$. Equation (6) reveals that the average afferent current depends linearly on the product of the thalamic rate and the transmission

¹The difference between this synaptic model and *averaged synaptic response* models of STD (Abbott et al. 1997; Tsodyks and Markram 1997), is that release and recovery are stochastic in one case and deterministic in the other. Neglecting the stochastic nature of the transmission leads to an underestimation of the fluctuations of the synaptic current and the post-synaptic response rate (de la Rocha and Parga 2005).

probability. The variance, σ^2 , which captures both the current stochasticity and its deterministic modulation [Fig. 1(c), right histogram], is basically determined by the peak-to-peak variations of $\mu(t)$. Therefore, changes in σ will have a big impact on the response firing rate.

2.5 Neuron model

We consider a single barrel neuron modeled as a leaky integrate-and-fire cell (LIF; Ricciardi 1977). The sub-threshold potential $V(t)$ of this cell obeys

$$C_m \frac{dV(t)}{dt} = -g_L(V(t) - E_L) + I_{\text{stim}}(t) + I_{\text{bg}}(t) \quad \text{if } V < \theta \quad (8)$$

where C_m is the total membrane capacitance, g_L is the leak conductance and E_L the leak potential. The membrane dynamics has a characteristic time constant defined as $\tau_m = C_m/g_L$. When the potential reaches a threshold value θ the neuron emits an action potential (AP) and $V(t)$ is reset at the value H where it remains during a refractory period of size τ_{ref} [see example in Fig. 1(e)].

2.6 Analysis of thalamic and cortical responses

We analyze the cortical response only once the *stationary* regime has been reached (i.e. after between 0.4 and 1 s). Most of this analysis will be done on the CSR, computed as the mean number of AP's emitted in a long time window divided by the window length. The CSR vs. the stimulation frequency will be referred to as the *response function*. The degree of phase-locking of spike responses to the periodic pattern of the stimulation, for both thalamic and cortical neurons, will be quantified with the vector strength (VS), defined as (Goldberg and Brown 1969):

$$VS = \frac{1}{n} \sqrt{\left(\sum_j \cos(2\pi f t_j) \right)^2 + \left(\sum_j \sin(2\pi f t_j) \right)^2} \quad (9)$$

where n is the total number of spikes and f is the frequency of the stimulation. This measure varies between zero, when there is no temporal alignment, and one, at perfect phase locking.

2.7 Simulations

Because the synaptic current is made of instantaneous pulses [Eq. (4)], mathematically described as Dirac delta functions, the evolution of the potential [Eq. (8)] can be solved in the simulations exactly. In contrast, the

generation of the spike trains with the inhomogeneous rate $\nu(t)$ does require a time binning which was taken as $dt = 0.05\text{--}0.005$ ms. The cortical neuron response was simulated for long enough periods (50–200 s of simulated time), and from three to five times, until when the standard error of the CSR and VS became approximately of the size of the symbols used in the plots. Thalamic PSTH's in all the figures were drawn using the corresponding analytical expressions. Traces of $P_t(t)$, $\mu(t)$ and the cortical PSTH's in Figs. 3 and 6 are drawn by the concatenation of a single period traces. The parameter values used in the model are given in the Appendix 1. All simulations were performed on a PC running under SUSE Linux. Most graphs were made using the free software plotting tool Grace.

3 Results

We analyze the TC transformations occurring in the model distinguishing between two different stimulation paradigms [Fig. 1(a)]:

- Repetitive pulse stimulation.
- Sinusoidal stimulation.

For each type of stimulation, we first present a model of the thalamic response and after analyze the cortical response. Because a full characterization of the transformations occurring in the pathway before the thalamus is beyond the scope of this study, we will make rather simple assumptions to characterize the thalamic response. Many of the filtering properties obtained in the cortical response will follow from the parameterization of the thalamic input, being synaptic depression and the membrane filtering the other two factors shaping these properties.

3.1 Repetitive pulse stimulation

3.1.1 Thalamic response

We start by defining a model of the thalamic response evoked by repetitive pulse stimulation of the vibrissae. In the absence of adaptation, increasing the stimulation frequency f implies reproducing the same thalamic response more frequently, such that the thalamic response to each deflection is independent of f [Fig. 2(b)]. Thus the mean number of spikes *per pulse* is constant, and the ThSR increases roughly linearly with the frequency [Fig. 2(c)].

The ThSR however does not provide any information about whether the temporal structure of the stimulus is represented in the thalamic discharges. A

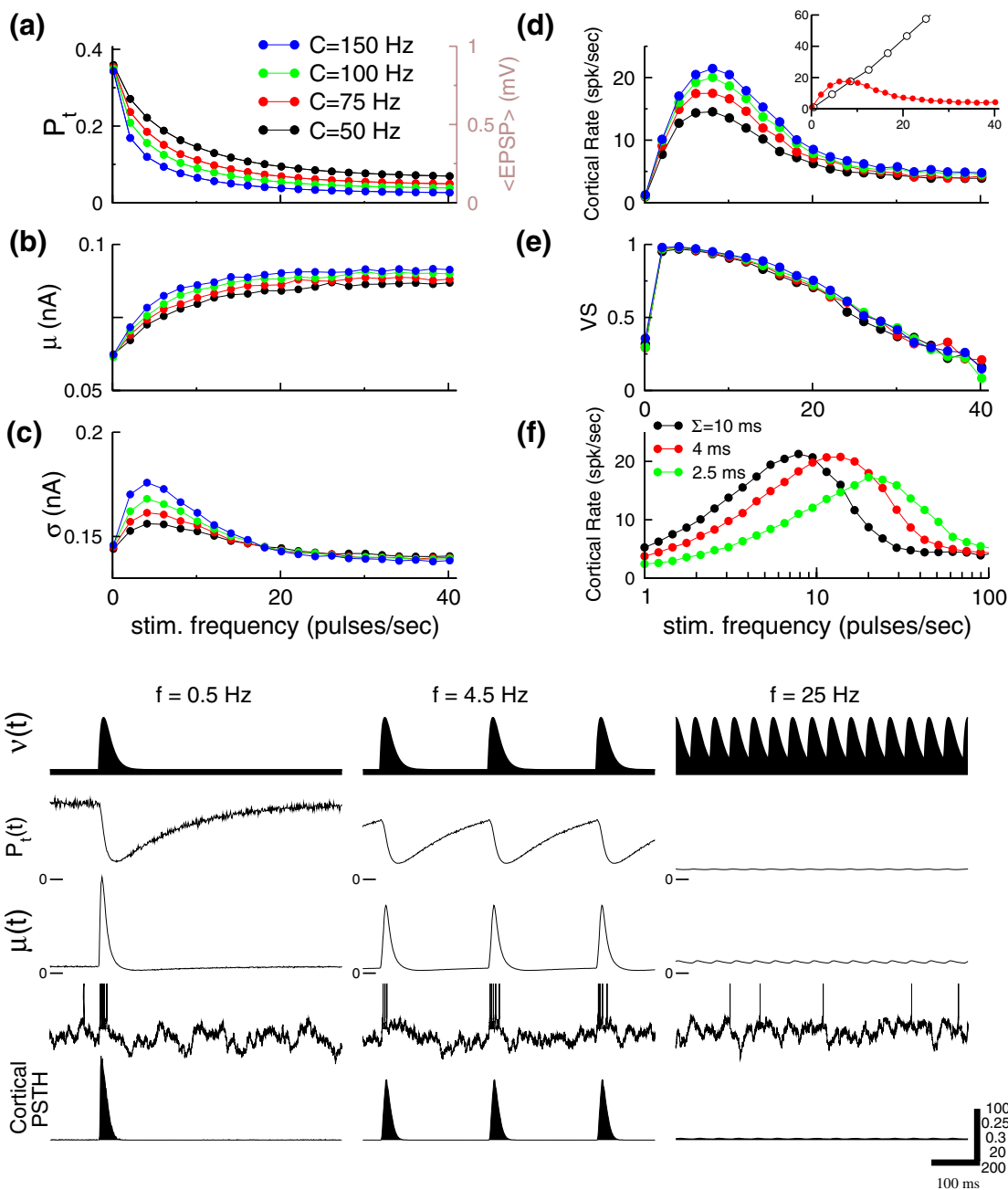


Fig. 3 Cortical response under repetitive pulse stimulation. *Top panels* transmission probability P_t (a), mean current μ (b), current deviation σ (c), CSR (d) and cortical VS (e) as a function of the frequency f , for different stimulation amplitudes [see legend in (a)]. (a) The probability P_t decreases with the frequency as $\frac{1}{f}$ (for high enough f). *Vertical axis on the right* shows the average EPSP amplitude corresponding to each value of P_t . (b–c) The $\frac{1}{f}$ behavior makes μ saturate and σ be non-monotonic. (d) This in turn endows the response with a band-pass behavior. *Open circles [inset in (d)]* illustrate one example ($C = 75$ Hz) with no depression: the rate follows a monotonically increasing trajectory. (e) the VS decreases substantially with f for frequencies beyond ~ 3 –4 Hz. (f) The band of transmitted frequencies depends on the pulse width Σ . *Bottom traces* in each

column show the temporal evolution of the instantaneous input rate (*top trace*), instantaneous transmission probability (*second trace*), mean instantaneous current (*third trace*), example voltage trace (*fourth trace*), and cortical PSTH (*bottom trace*) for a particular stimulus frequency (see labels above the traces). Filtering at $f = 25$ Hz occurs because $P_t(t)$ is maintained at very low values due to the high afferent spike rate. Thus, the synaptic current produced by a single pulse is too small and makes unlikely that the neuron reaches threshold. Parameters: $\tau_m = 10$ ms (a–e) and 5 ms (f). $\theta = 17$ mV [except in (f) $\theta = 10$ mV], $H = 10$ mV [except in (f) $H = 6$ mV], $\Sigma = 10$ ms. $C = 160$ Hz in (f), and $C = 125$ Hz in all *bottom traces*. The others are as indicated in Appendix 1

commonly used variable for quantifying the degree of phase locking of the spikes is the vector strength (VS) (see Section 2). The VS is related with the shape of the *phase histogram* (PH), which is the same as the CPSTH where the time units have been replaced with phase units [Fig. 1(b) right]. A VS equal to zero means a uniform PH, meaning that spikes occur with equal probability at any phase. A value of VS close to one means a PH narrowly peaked around a particular temporal phase, and zero elsewhere. Thus, the value of the VS is determined by two distinct factors: (1) the width of the PH peak, so that the wider the peak the smaller the VS; and (2) the ratio between the area under the peak and the total area. Ideally, this ratio measures the fraction of spikes triggered by the stimulus.

When using repetitive pulse stimulation, increasing f alters these two magnitudes in opposite directions: (1) increasing the PH peak width, since the constant temporal width of the response, Σ , represents a wider range of phases. This makes the VS decrease. (2) increasing the fraction of spikes which are triggered by the stimulus, since the number of stimulus-asynchronous spikes, those generated by the basal rate, decreases as $\frac{v_0}{f}$. This makes the VS increase.

The behavior of VS vs. f depends ultimately on the specific values of v_0 , Σ and C which determine the relative weight of these opposing effects: (1) if for instance $v_0 = 0$ there are no stimulus-asynchronous spikes, the mentioned fraction is always one and the VS decreases monotonically with f [Fig. 2(d) black circles]. (2) In contrast, if $v_0 = 20$ Hz and the width of the Gamma is small (e.g. $\Sigma = 2$ ms), the VS increases monotonically in the range $f \sim 0$ –40 Hz because the second effect prevails [Fig. 2(d) blue circles]. For the values chosen in what follows ($v_0 = 5$ –10 Hz, $\Sigma = 10$ ms and $C = 50$ –150 Hz), the behavior of the VS is band-pass with a maximum around $f \sim 10$ Hz, meaning that both effects have an impact [Fig. 2(d) red circles].

A final important point is that under stimulation with repetitive pulses the velocity of the whisker does not change with the applied frequency simply because the shape of the pulse remains fixed. This is the reason why no reference was made here to velocity encoding in the thalamus.

3.1.2 Cortical response

The transmission probability P_t decreases as the stimulation frequency increases [Fig. 3(a)]. This happens because as f increases more spikes reach the synapses

per unit time depleting the bouton of vesicles. Beyond a limiting frequency the synapses enter into the saturation regime where P_t decreases as $\frac{1}{f}$ (Abbott et al. 1997; Tsodyks and Markram 1997) causing the mean current μ to saturate [Fig. 3(b)]. The variance of the current, σ^2 , behaves non-monotonically [Fig. 3(c)]. This occurs because at low frequency the peaks of $\mu(t)$ are large but temporally sparse while at high frequencies they are very small due to depression (bottom traces in Fig. 3, left and right columns respectively). Only at moderate frequencies, σ achieves a maximum, resulting from the compromise between the number of peaks per unit time and their amplitude (bottom traces in Fig. 3, center).

The CSR shows a similar band-pass behavior with a preferred frequency f_p around ~ 8 Hz. High frequencies are therefore filtered due to depression. Increasing the stimulation amplitude, C , increases the overall non-monotonic response with no shift of the preferred frequency [Fig. 3(d)]. However, this increase rapidly saturates (compare blue and green circles in the figure). Again, because of TC depression, the peak of the instantaneous afferent current does not increase linearly with C . In the absence of depression, the CSR increases monotonically with f showing that depression is needed in order to filter high frequency pulses [Fig. 3(d) inset, open circles].

While changes in C do not alter considerably neither the size nor the position of the band of transmitted frequencies [see Fig. 3(d)], decreasing Σ shifts the whole response curve to higher frequencies [Fig. 3(f)]. This is occurs because shorter thalamic responses are less effective driving a cortical response so that CSR decreases for low frequencies. Moreover, because of fewer thalamic spikes per deflection, the suppressive effect of STD kicks in at higher f yielding a shift of the transmitted band to higher frequencies.

The cortical VS exhibits a non-monotonic shape with a maximum around $f \sim 5$ Hz [Fig. 3(e)]. At low f , the CSR is small and close to its spontaneous value (~ 3 Hz). Thus, the AP's triggered by the stimulus are therefore a small fraction of the total yielding a small VS (see above). The decreases of the thalamic VS [Fig. 2(d) red circles] causes the decrease of the cortical VS for $f > 5$ Hz.

3.1.3 Thalamic and cortical responses with frequency adaptation

We consider the effect of thalamic adaptation, defined as the decrease of the peak thalamic response, C , with

stimulation frequency (Ahissar et al. 2000; Hartings et al. 2003; Castro-Alamancos 2002), which we model with the following dependence:

$$C(f) = \frac{C_0}{1 + \alpha f} \tag{10}$$

Here C_0 represents the amplitude at zero frequency, the *adaptation susceptibility* α quantifies the strength of adaptation and f is given in pulses per second. A value $\alpha = 0$ implies no adaptation (the case considered in Fig. 3) while $\alpha = 1$ implies very strong adaptation [Fig. 4(a)]. Figure 4(b) illustrates that up to $\alpha = 0.05$, which corresponds to a suppression of the thalamic amplitude of 2/3 at $f = 40$ pulses/s, there is very little change in the CSR with respect to the case with no

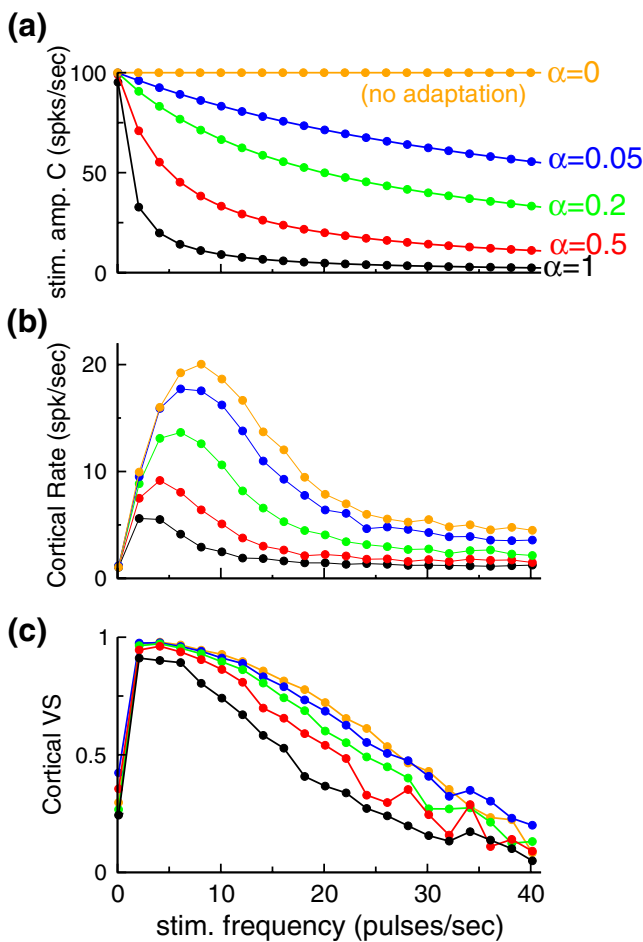


Fig. 4 Cortical response under repetitive pulse stimulation with thalamic adaptation. (a) Thalamic rate amplitude C vs. stimulation frequency for several adaptation susceptibilities (see labels over curves). (b) CSR vs. f shows that up to substantial adaptation susceptibility, $\alpha = 0.05$, the response function almost does not vary with respect to the case with no adaptation. Larger susceptibilities bring down the CSR until eventually it is suppressed. (c) Cortical VS vs. f . Labels in (a) apply to all plots. Parameters are as in Fig. 3

adaptation [Fig. 4(b)]. With stronger adaptation susceptibilities, the CSR still shows a band-pass behavior but it peaks at a lower f . When α is very large, the CSR is equal to spontaneous activity at any f .

3.2 Sinusoidal stimulation

Motivated by experiments reporting an increase of the CSR with f up to $f \sim 340$ Hz when using a sinusoidal whisker stimulation (Arabzadeh et al. 2003), we explore whether a sinusoidal stimulus may be encoded in VPM in a different way such that STD does not suppress the response at high frequencies. To achieve this, the synapses must not depress as f increases therefore avoiding that high frequency pulses are filtered. We propose that, under sinusoidal stimulation, the thalamic spike rate remains invariant to changes in f (see Section 4). This rather speculative assumption is based on limited data reporting a small ($\sim 20\%$) increase of the ThSP in the interval $f = 0-40$ Hz. The rationale for this assumption is that the level of depression will be invariant to changes in f . This is obtained by making the area of the CPSTH scale with the frequency as $\frac{1}{f}$, similarly to the area under one sinusoidal cycle. In addition, the CPSTH area must grow linearly with the stimulation amplitude, A . The two assumptions are formalized in the scaling relation

$$C \Sigma \propto \frac{A}{f} \tag{11}$$

In contrast to the pulse stimulation, changing f using sinusoidal stimulation changes the velocity of the whisker. In addition, some experiments seem to indicate that the velocity is encoded in VPM (Pinto et al. 2000). We will therefore analyze two different parameterizations of the thalamic response following the scaling in Eq. (11):

- Without velocity encoding in VPM
- With velocity encoding in VPM

The analysis of the first case will allow us to understand better the impact that encoding the velocity in the thalamus has on the cortical response.

3.3 Sinusoidal stimulation without velocity encoding

3.3.1 Thalamic response without velocity encoding

In the absence of velocity encoding in the thalamic response, we make the natural assumption that the CPSTH amplitude depends only on the stimulation

amplitude and its temporal width scales linearly with the cycle period:

$$C \propto A \quad \Sigma \propto \frac{1}{f} \quad (12)$$

Figure 5(b) illustrates the thalamic PSTH obtained in this case for several frequencies and amplitudes. The mean number of spikes per deflection decreases as $\frac{1}{f}$ making the ThSR invariant with f [Fig. 5(d)]. This scaling gives qualitatively similar results to the case

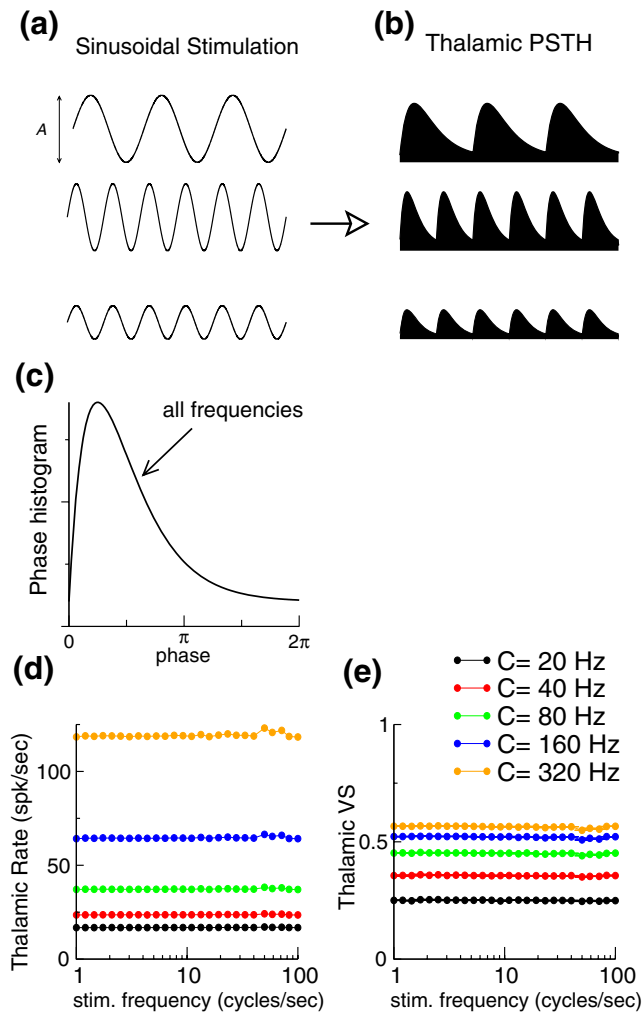


Fig. 5 Thalamic response under sinusoidal stimulation *without* velocity encoding. (a–b) three example stimuli (a) and the corresponding PSTH’s (b), according to our model of the VPM response without velocity encoding. The time to peak Σ scales proportionally to the cycle period (i.e. as $\frac{1}{f}$). The peak response C depends solely on the stimulus amplitude A . (c) The scaling of the response width leads to a phase histogram independent of the frequency. (d) The rate is independent of f as well because the number of AP’s per cycle decreases as $\frac{1}{f}$. (e) The VS is constant as a consequence of the invariance of the phase histogram with the frequency. Parameters: $\Sigma = 0.125/f$ in (c–e). The other parameters are as indicated in Appendix 1

where the VPM activity is modeled as a rectified version of a sine wave (data not shown). It also has the property that, under changes in f , the spikes remain equally distributed across temporal phases [Fig. 5(c)] yielding a constant thalamic VS [Fig. 5(e)].

3.3.2 Cortical response without velocity encoding in VPM

The CSR vs. f shows a band-pass behavior with a preferred frequency at ~ 10 Hz [Fig. 6(d)]. Larger amplitudes give rise to larger response rates, but this increase saturates due to STD. When there is no depression, the response shows a low-pass behavior and it overlaps the case with depression at high frequencies [Fig. 6(b–e), open symbols]. This reveals that depression does not filter the response at high frequency [note that P_t does not decrease with increasing frequency; Fig. 6(a)]. The filtering here is attributable to the passive properties of the cell membrane (Koch 1999): because of the membrane capacitance, the cell integrates the synaptic current as an RC electric circuit and it behaves as a low-pass filter.

What is then the effect of STD on the response? Depression suppresses the cortical response at *low frequencies* [Fig. 6(d)]. This suppression causes σ to be smaller when there is depression [Fig. 6(c) compare full and open circles]. The decrease of σ reflects the decrease of the peak amplitude of the current at low f [Fig. 6(f) left column]. This happens because the time to peak of the thalamic response is very large at low f ($\Sigma = 250$ ms in the example $f = 0.5$ Hz; top left trace) which causes the synapses to get depleted before the thalamic rate peaks. This is shown in the rapid drop of $P_t(t)$ [Fig. 6(f) left]. This “early” synaptic depression produces a $\mu(t)$ with phase-advanced small peaks which generate a low cortical response (Chance et al. 1998). In contrast, at higher frequencies fewer spikes arrive before the maximum and they are less effective because $P_t(t)$ does not recover so much between cycles [Fig. 6(f), see $f = 10$ and 50 Hz traces]. This makes $\mu(t)$ to peak almost simultaneously with the thalamic rate (i.e. little phase advance), thus having a larger amplitude. As f increases further, $P_t(t)$ becomes approximately constant because of a disassociation of the depression and input time scales. This causes the instantaneous mean current to be the same as the thalamic signal times a constant factor, i.e. $\mu(t) \propto v(t) P_t$, [Fig. 6(f) right column].

The cortical VS shows a wide band-pass behavior with a maximum around ~ 5 Hz [Fig. 6(e)]. This occurs because, at low and high frequencies the CSR is low and comparable to the spontaneous rate.

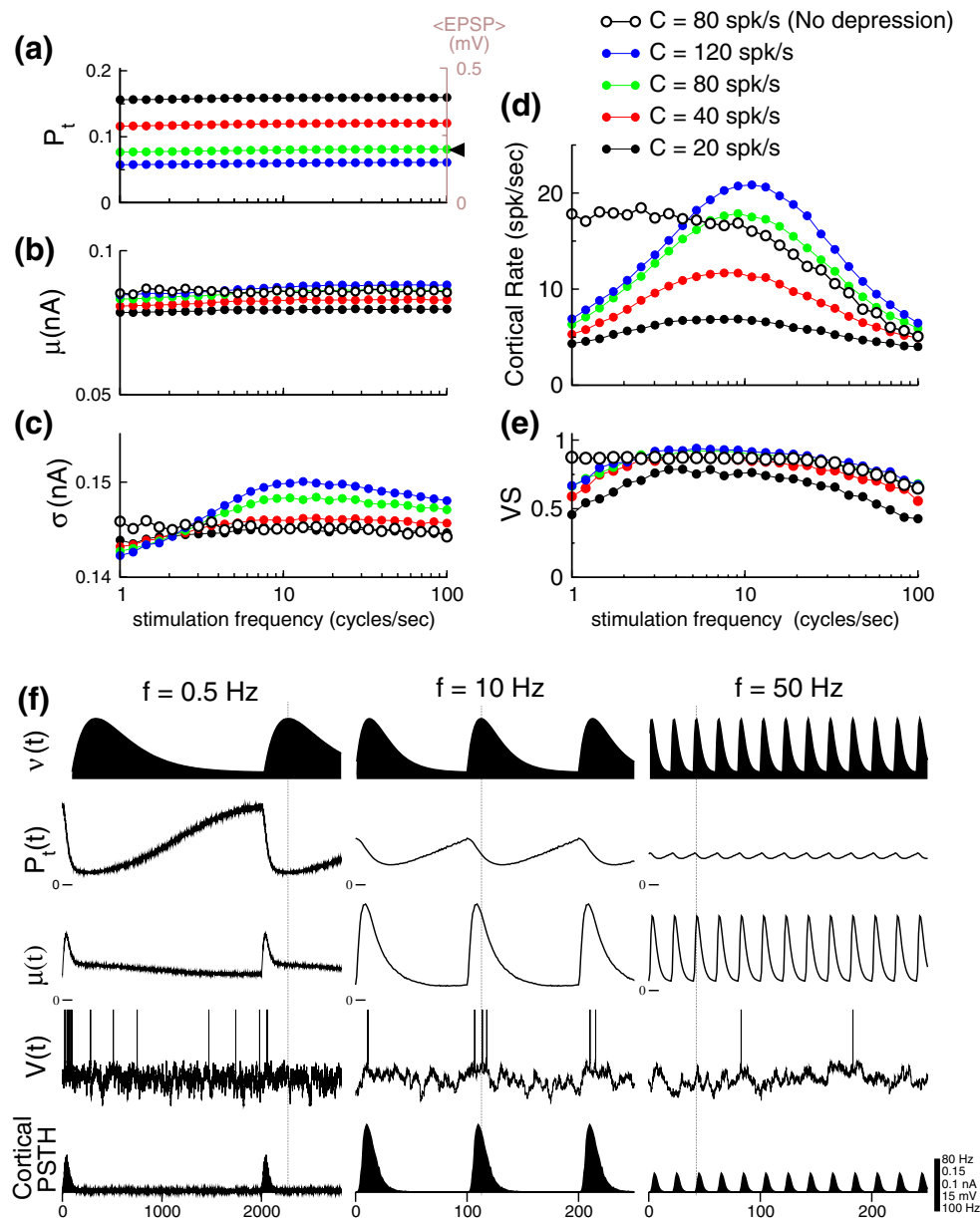


Fig. 6 Cortical response under sinusoidal stimulation *without* velocity encoding in VPM. The transmission probability (a), mean current (b), current deviation (c), cortical rate (d) and VS (e) are shown as a function of the frequency, f , for several values of the amplitude C (top legend applies to all plots). A case without depression is also shown for comparison (*open circles*). (a) In contrast to the repetitive pulse stimulation [Fig. 3(a)], the transmission probability of the TC synapses is independent of f because in this model the ThSR is independent of f [Fig. 5(c)]. *Arrowhead* indicates the constant P_t for the case without depression. (b) The mean current remains essentially constant due to the constant behavior of P_t . *Vertical axis on the right* shows the average EPSP amplitude corresponding to each value of P_t . (c) The current variance, σ^2 , shows a moderate increase at low f if there is STD and it remains constant in the case without depression. (d) With STD the cortical rate shows a band-pass behavior, for all amplitudes. Without depression it exhibits a low-pass behavior revealing that high frequencies are not filtered

by STD but by the membrane. Thus only the filtering of low frequencies is attributable to STD. (e) The VS has a rather wide band-pass behavior taking high values in the range of frequencies where the neuron responds best. (f) Instantaneous thalamic rate (*top trace*), $P_t(t)$ (*second trace*), $\mu(t)$ (*third trace*), example voltage trace (*fourth trace*) and cortical PSTH (*bottom trace*) for three frequency values (see labels on top of each column). As in the case of repetitive pulses, the $P(t)$ trace tends to a constant value as f grows, but in contrast to that case this value is not zero. Because of this, the trace of $\mu(t)$ is not damped and follows well the input $v(t)$ at high f . Despite of this the response is reduced at $f = 50$ Hz. *Vertical dotted lines* serve to illustrate the phase advanced response at low f . Check the different time scale used in the traces with $f = 0.5$ Hz. Parameters: $U = 0.08$ for the non-depressing example in (c); $\tau_m = 5$ ms, $\theta = 10$ mV, $H = 6$ mV; $C = 80$ Hz (in all traces); $\Sigma = \frac{0.125}{f}$. The rest as indicated in Appendix 1

3.4 Sinusoidal stimulation with velocity encoding

3.4.1 Thalamic response with velocity encoding

The assumption of constant ThSR with f avoids the suppression of high frequencies by STD, yet it is not sufficient to obtain a high-pass behavior in our barrel

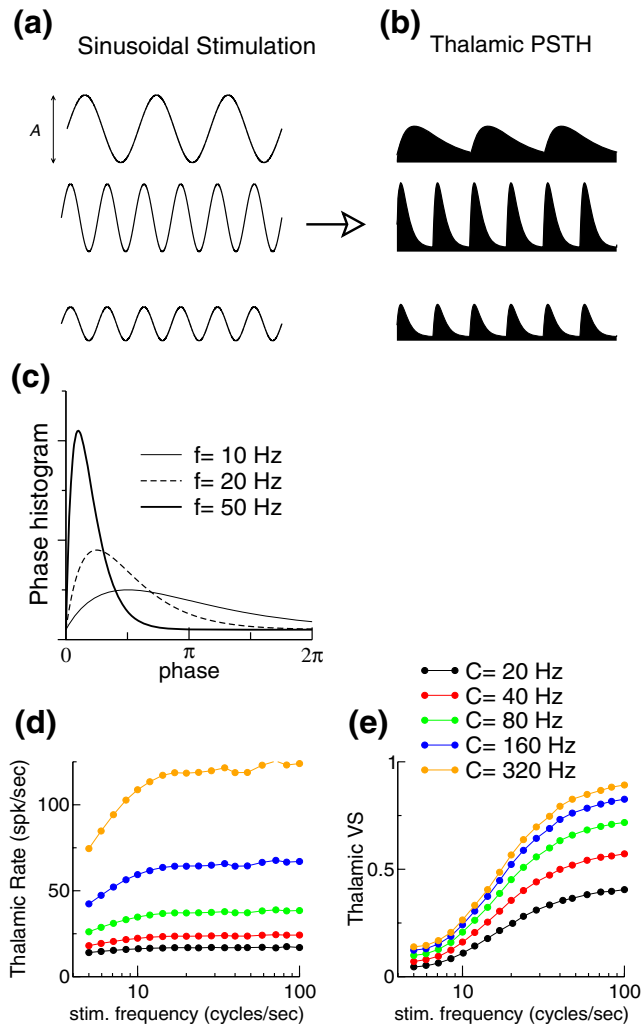


Fig. 7 Thalamic response under sinusoidal stimulation *with* velocity encoding. **(a–b)** three example stimuli **(a)** and the corresponding PSTH's, according to our model of the VPM response where the whisker velocity, Af , is encoded in the temporal contrast (i.e. $C \propto Af$, and $\Sigma \propto \frac{1}{f^2}$). **(c)** The phase histogram shows that higher frequencies produce responses with higher temporal contrast, i.e. more skewed responses with higher peaks. **(d)** The rate shows a slight increase at low f 's (because of the truncation of the Gamma function at low f) and becomes basically constant at intermediate frequencies because the number of spikes per cycle decreases as $\frac{1}{f}$. **(e)** The VS increases monotonically with f as a result of higher frequencies producing more precisely phase-locked responses. Parameters: $\Sigma = 2.5\text{Hz}/f^2$ (f in hertz) in **(c–e)**

cell. We thus explore a different parameterization of the thalamic response which has constant ThSR and encodes the stimulus velocity.

Our parametrization of the thalamic response is based on experimental findings showing that the stimulus velocity is encoded in the *temporal contrast* of the VPM response (Pinto et al. 2000). This implies that higher velocities lead to a temporal redistribution of the spikes which tend to be discharged more synchronously at the stimulus onset (see Appendix 2). Thus, in our model (1) the ThSR is still invariant with f , as expressed previously in Eq. (11). In addition, (2) the *mean velocity* is encoded linearly in the temporal contrast of the VPM activity, which in the case of a Gamma-shaped CPSTH equals the amplitude C (see Appendix 2). Putting these two assumptions together we conclude that

$$C \propto Af \quad \Sigma \propto \frac{1}{f^2} . \quad (13)$$

Under this scaling the thalamic VS increases monotonically with the frequency [Fig. 7(e)]: a greater velocity increases the temporal contrast of the response, implying that VPM spikes cluster closer to the response onset and therefore are more precisely phase locked. This can be observed in the phase histogram in Fig. 7(c) and it is noticeable, although more subtle, in the thalamic PSTH's [compare the scaling of the PSTH with f in Fig. 5(a–b) with Fig. 7(a–b)].

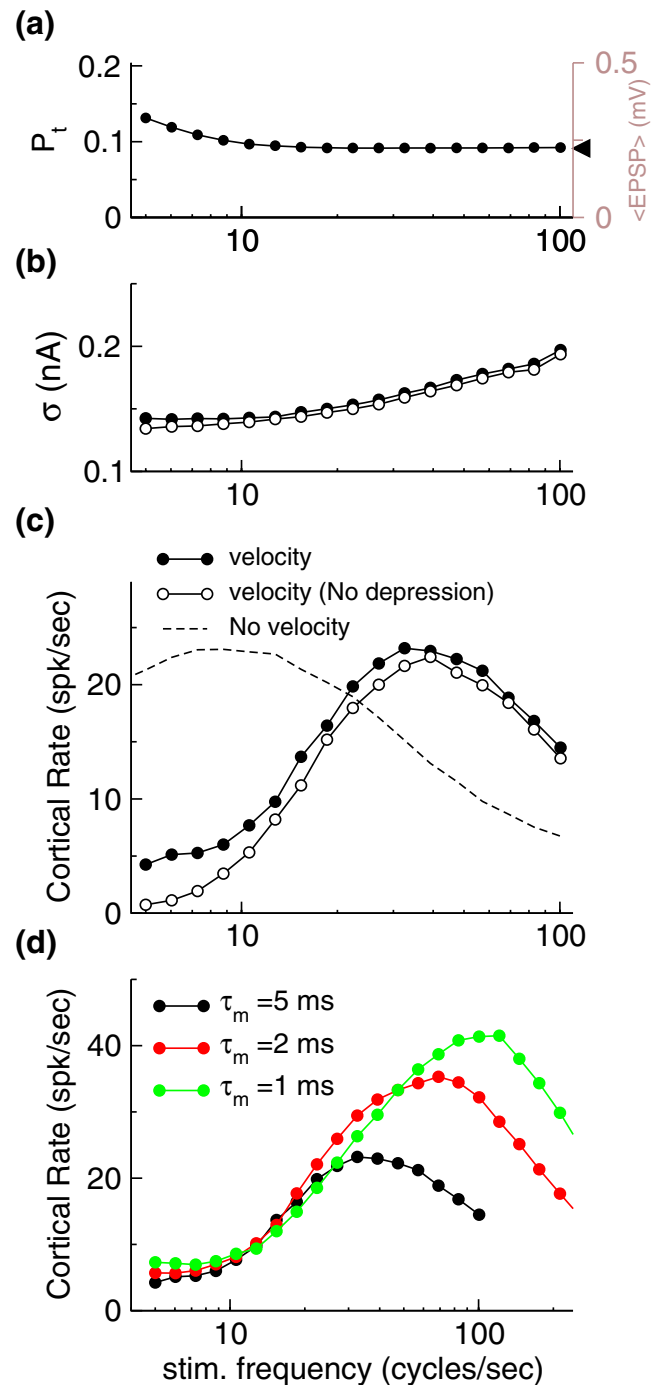
3.4.2 Cortical response with velocity encoding in VPM

When the velocity is encoded in VPM, the cortical response function undergoes a substantial shift to higher frequencies: the CSR starts rising at a higher f , peaks around 50 Hz and then falls off [Fig. 8(c)]. This shift is a consequence of the increase in the peak current with f [Fig. 8(b)], which follows from the linear increase of the peak of the thalamic response [Eq. (13)]. At low f , the thalamic peak responses are so small that they produce almost no cortical response and the CSR equals the spontaneous rate. As f increases, higher current peaks elicit higher cortical rates until, at relatively high f , the passive properties of the membrane bring down the response. Thus, although the membrane still filters high frequencies, the encoding of the velocity counteracts this effect and allows the neuron to respond up to higher frequencies. Comparing the cases with and without STD shows that depression does not contribute to shape the response function much, since

Fig. 8 Cortical response under sinusoidal stimulation with velocity encoding in VPM. **(a)** The transmission probability is essentially constant for all f (arrowhead indicates the constant P_t for the case without depression). Vertical axis on the right shows the average EPSP amplitude. **(b)** the current variance grows with f reflecting the increase of the peak thalamic response which varies as $C \propto f$. The cases with and without (open circles) depression overlap for all f . The mean current is not shown because it presents the same constant behavior as in Fig. 6(b). **(c)** The CSR is compared in the cases of (1) velocity encoding with depression, (2) velocity encoding without depression and (3) with depression but without velocity encoding. In all cases, the CSR has a band-pass behavior but encoding the velocity dramatically shifts the band of transmitted frequencies towards higher values. The examples with and without depression overlap at almost all frequencies revealing that filtering, neither at low nor at high frequencies, is attributable to depression. At low frequencies, the response is low because the current variance is small **(b)**. High frequencies are filtered by the membrane, which works as a low-pass filter. **(d)** The CSR is compared for decreasing values of τ_m : the raising part of the response function expands to higher frequencies as τ_m decreases. Parameters: $\Sigma = \frac{2.5}{f^2}$ (f is in hertz). P_t and σ are both independent of τ_m . Other parameters are as in Fig. 6 except that in **(c)**: $\tau_m = 2$ ms, $\theta = 7$ mV, $H = 4$ mV, $v_E = 7.41$ ms⁻¹, $v_I = 1.1$ ms⁻¹ (red symbols); $\tau_m = 1$ ms, $\theta = 6$ mV, $H = 3$ mV, $v_E = 11.97$ ms⁻¹, $v_I = 1.24$ ms⁻¹ (green symbols). $U = 0.09$ for the non-depressing example in **(b-c)**. Legend in **(c)** applies for the plots **(a-c)**

the CSR in both cases overlap at almost all frequencies [Fig. 8(c)].

The fall-off of the CSR at high frequency is dictated by the value of the membrane time constant which equals the membrane capacitance divided by the total membrane conductance. It has been shown that network synaptic activity may substantially increase the total conductance of a cell both *in vivo* (Borg-Graham et al. 1998; Hirsch et al. 1998) and *in vitro* (Chance et al. 2002). This results in an effective membrane time constants of a few milliseconds. Because our cell model is not conductance based, we investigate the impact of an *ad hoc* decrease of τ_m on the response of the barrel cell. Along with the decrease in τ_m we mimic the increase in network synaptic activity by increasing the background rates v_E and v_I . Going down to the limit case of $\tau_m = 1$ ms the CSR increases monotonically up to a preferred frequency of $f_p \sim 100$ Hz [Fig. 8(d)]. However, the cortical neuron still has a band-pass response when explored in a large enough frequency range. Therefore, although the encoding of the velocity along with a decrease of the membrane time constant enables the neuron to respond up to higher frequencies, it does not overcome the eventual fall-off of the CSR due to the integration properties of the membrane. Finally, the VS shows a monotonically increasing behavior up to ~ 100 Hz where it slowly starts to drop off (data not shown).



3.4.3 Can the cortical response encode the velocity?

Arabzadeh et al. (2003) found that the CSR of clusters of cells encode the product $A \times f$ more optimally than the amplitude or the frequency independently. To test to what extent our model can reproduce this result, we have computed the CSR for a number of different frequencies and amplitudes equally spaced

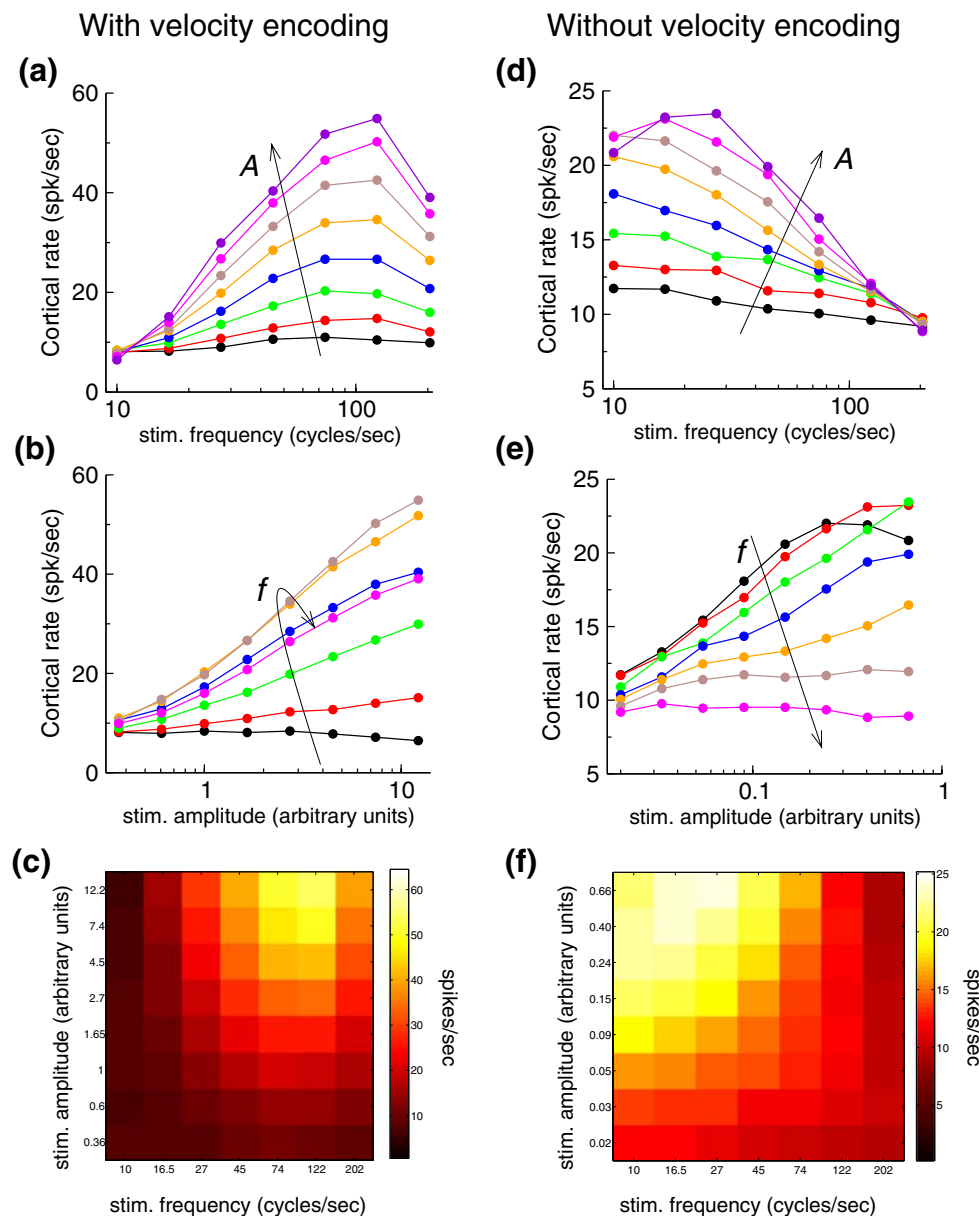


Fig. 9 Encoding of the stimulus velocity in barrel cortex. Cortical rate curves are drawn for different frequencies and amplitudes in the case with (a–c) and without (d–f) velocity encoding. *With velocity encoding:* (a) the CSR is plotted vs. frequency for several amplitudes (amplitudes increase from bottom to top following the superimposed arrow). Constraining the frequency range to $20 < f < 120$ the response shows a monotonic increase with both the frequency and amplitude. Beyond this range the response decays due to the passive properties of the membrane. (b) The same data set shown in A is plotted here as CSR vs. amplitude. The frequencies 10, 16.5, 27, 45, 74 and 122 Hz increase from bottom to top, while the highest 202 Hz coincides with $f = 74$ Hz (see arrow). (c) The same data is shown in a color plot.

Perfect encoding of velocity would result in a plot where the tiles along the diagonals (from top left to bottom right) are of the same color. The encoding within the mentioned frequency range (see superimposed box), albeit not perfect, is reasonable. *Without velocity encoding:* (d–f) The same type of plots as in (a–c) are shown for the case in which the thalamic cells do not encode the velocity. The encoding of the velocity in the cortical rate becomes now impossible for any range of the frequency. Parameters: $\tau_m = 1$ ms, $\Sigma = 5\text{Hz}/f^2$ (f in hertz) in (a–c) and $\Sigma = 0.125/f$ in (d–f). Amplitude values set the constant of proportionality of $C \propto f$ in (a–c) and the amplitude C in spike/ms in (d–f). The rest of the parameters are as in Fig. 8(d)

in the plane $A - f$, whose values are comparable to those employed in the quoted study. We have then represented the same set of data in three different ways:

(1) CSR vs. frequency [Fig. 9(a)]; (2) CSR vs. amplitude [Fig. 9(b)] and (3) CSR vs frequency and amplitude in a color plot [Fig. 9(c)]. This is the same representation

used in (Arabzadeh et al. 2003) so that the results can be directly compared.

Figure 9(a–b) illustrate that in the range $15 < f < 120$ Hz the CSR increases monotonically with either the frequency or the amplitude, showing a qualitative agreement with the experiments. At higher frequencies ($f > 120$ Hz) the membrane filtering drops the response in disagreement with the mentioned experiments. A different question is whether the CSR is uniquely determined by the product $A \times f$. If this property was perfectly true Fig. 9(c) would show that the tiles along each iso-velocity diagonal, i.e. those from top left to bottom right, have the same color. Different iso-velocity diagonals would show different colors. The actual results show that within the frequency range mentioned above, although not perfect, the encoding is approximately valid. This result is specially relevant when it is compared with the one obtained using the thalamic response model with no velocity encoding [Fig. 9(d–f)]. Using this model, because the CSR essentially decreases with f in the explored range [Fig. 9(d)], the diagonals with approximately constant rate are orthogonal to the iso-velocity diagonals [Fig. 9(f)]. Thus the CSR seem to be encoding more the ratio A/f than the product $A \times f$.

In summary, the strategy of encoding the velocity in the temporal distribution of the thalamic spikes has two major implications: (1) it makes the ThSR to be constant preventing the depression of TC synapses, and the subsequent suppression of the cortical response, as the frequency increases; (2) the CSR increases monotonically up to much higher frequencies and approximately encodes the velocity. However, the redistribution of spikes at high velocities implies very fast modulations of the afferent current which are eventually filtered by the membrane capacitance. This suggests that extra neural or cortical circuit mechanisms not considered here are required for encoding the velocity up to the highest frequencies employed in the mentioned experiment (Arabzadeh et al. 2003).

4 Discussion

4.1 Different response properties to sinusoidal and repetitive pulse stimulation

The response of cortical neurons across frequencies depends crucially on whether the stimulation is sinusoidal or a repetitive application of fixed pulses. With pulses, the suppression of the cortical response with increasing frequency is produced by TC depression (Fig. 3). The frequency at which the CSR peaks, f_p , was found to

decrease with the temporal width of the thalamic input [Fig. 3(f)]. Because this width depends on the pulse duration (Sosnik et al. 2001), we predict that shorter pulse stimuli should give rise to a higher f_p .

If the stimulus is sinusoidal, the ThSR is constant and the mean level of depression is invariant with f . Nevertheless, high frequencies are still filtered due to the passive properties of the cell membrane, which behaves as a low-pass filter [Fig. 6(d)]. Thus, while high frequencies are filtered by the membrane, STD is responsible for the filtering of low frequencies (Chance et al. 1998). Considering the increase in whisker velocity with the sine frequency, causes the temporal contrast of the thalamic response to increase with f . This, shifts and stretches the band of transmitted frequencies to higher values. In spite of this, very high f 's are still filtered by the membrane. In summary, the simplest coding of a sinusoidal stimulus in the thalamic response also produces a cortical band-pass behavior, although it appears for different reasons.

4.2 Contrasting our hypothesis about the thalamic response

We now evaluate how realistic is our modeling of the thalamic response when compared with the available experimental data. Recordings of VPM cells applying different types of pulse stimulation found that the CPSTH shows little adaptation with f in the range of moderate frequencies (e.g. ~ 15 – 20% at $f \sim 30$ Hz) (Hartings and Simons 1998; Hartings et al. 2003; Sosnik et al. 2001). Another important study reveals that during quiescent states, thalamic responses to repetitive whisker stimulation are strongly suppressed at frequencies above $f \sim 2$ Hz. In contrast, during activated states VPM cells respond sustainably at least up to $f = 40$ Hz (Castro-Alamancos 2002). Since the data is not conclusive about the extent of thalamic adaptation *in vivo*, we have first neglected adaptation, and then considered the case of an arbitrary adaptation susceptibility (Fig. 4).

Both pulses and sinusoidal stimulation evoke thalamic responses which resemble a Gamma function (Sosnik et al. 2001; Hartings et al. 2003; Khatri et al. 2004). Moreover, thalamic CPSTH's in response to high f sinusoidal stimulation show a secondary smaller peak which we neglected [probably produced by inhibition coming from reticular cells (Golomb et al. 2006)]. The results shown in this letter however, are not contingent on the specific shape of the CPSTH but essentially on its scaling with f and A .

More speculative is the assumption that, under sinusoidal stimulation, the ThSR is invariant with f .

The available data is limited to the interval $f = 0$ –40 Hz where it increases by about 20% (Khatri et al. 2004; Hartings et al. 2003). Based on this, we take the extreme assumption that the ThSR remains constant in the whole interval $f = 0$ –200 Hz. This, allowed us to find out that STD can have a very different impact on the response function, in fact almost none, when the ThSR does not increase with f .

The encoding of the whisker velocity in the whisker–barrel system has been analyzed in several studies (Welker et al. 1964; Lichtenstein et al. 1990; Shoykhet et al. 2000; Pinto et al. 2000; Arabzadeh et al. 2003). In particular, in a study of the VPM response to single ramp-and-hold pulses, Pinto et al. (2000) observed that changes in the slope of the ramp (i.e. the velocity) produced a linear increase in the *temporal contrast* of the VPM response with little variation in the number of discharges. This is equivalent to a temporal redistribution of the spikes which tend to be discharged more synchronously at the onset (see Appendix 2). Given that the encoding of the velocity in the barrels has been observed up to very high frequencies (340 Hz) (Arabzadeh et al. 2003), we have assumed that VPM cells must also encode the velocity in their temporal contrast in this whole range. By doing this, we have explored an alternative strategy to encode a sinusoidal stimulus different to the standard rectified sine used in previous modeling studies (see e.g. Chance et al. 1998; Carandini et al. 2001).

4.3 Comparison of the cortical response of the model with experiments

Experiments probing the barrel response using low and high frequencies have led to seemingly contradictory results: repetitive pulses at moderate frequencies give rise to a band-pass behavior of the CSR (Garabedian et al. 2003), while sinusoidal stimulation produces a monotonous increase of the CSR up to very high frequencies (~ 350 Hz) (Arabzadeh et al. 2003). Our results can help to clarify this apparent contradiction, by showing that one must carefully distinguish between repetitive and sinusoidal stimulation because: (1) at high frequencies depression of TC synapses suppresses the response in the first, while it plays no role in the second; (2) only under sinusoidal stimulation the whisker velocity changes with the frequency, something that facilitates the response at higher frequencies.

The band-pass response function obtained in our model using pulses agrees with experimental data obtained using the same kind of repetitive pulse stimulation (Garabedian et al. 2003). Including moderate levels of thalamic adaptation has little impact on the

response since it is mainly determined by the depression of TC synapses [Fig. 4(a)]. The VS obtained in the model with moderate adaptation [Fig. 4(c)] matches that obtained in the mentioned study, namely a band-pass behavior with maximum around $f \sim 5$ Hz (Garabedian et al. 2003).

Fewer studies measuring the response of barrel cells have employed sinusoidal stimulation (Hartings et al. 2003; Arabzadeh et al. 2003; Khatri et al. 2004). As mentioned above, Arabzadeh *et al* found that the CSR increases *monotonically* with the frequency up to $f \sim 340$ Hz (Arabzadeh et al. 2003). In addition, these cells encode the mean velocity of the stimulus, Af , in their rate. In a recent study, using lightly narcotized animals, Khatri et al. (2004) found that the CSR is basically insensitive to the stimulus frequency in the interval $12 < f < 40$ Hz. It is likely that differences in anesthesia, stimulus velocity values, the number of stimulated whiskers and the different frequency interval used underly these major discrepancies.

We have used the model of thalamic response described above to test whether we could reproduce the results obtained in (Arabzadeh et al. 2003). We found that, when the velocity is encoded in VPM, the CSR increases monotonically up to high frequencies [compare Fig. 6(d) with Fig. 8(c)]. Its ability to encode the velocity in the barrel rate appears quite remarkable when the CSR is plotted vs frequency and amplitude and compared with the case where there is no velocity encoding in the thalamus [Fig. 9(c and f)]. However, this oversimplified model cannot avoid that at frequencies beyond 100 Hz, the passive properties of the neuron membrane dominate and the response drops off [Fig. 8(c and d)]. As a consequence, the CSR can only encode the velocity in a limited frequency range, i.e. 15–100 Hz.

Obviously, the lack of intra-cortical interactions in the model must be one of the major causes of this disagreement. An indication that the cortical network has an important effect on the neuron response is that data shows that cortical cells are not phase-locked to the signal (Arabzadeh et al. 2003), meaning a negligible VS (in contrast to the larger VS observed under stimulation with repetitive pulses (Garabedian et al. 2003)). Given that VPM discharges are precisely locked to a sine stimulus up to 300 Hz (Deschenes et al. 2003), the lack of phase locking in the barrels reveals that the cortical activity has not inherited the precise phase-locked character of its input, possibly because the cortical circuit generates stimulus-asynchronous synaptic currents onto the recorded neuron and/or because long lasting recurrent NMDA conductances play a major role driving the neuron response (Fleidervish et al.

1998). A recent theoretical study has shown that feedback decreases the temporal reliability of the neural response (Lin et al. 2007; although see Bazhenov et al. 2005 where reliability might increase at low frequencies and small amplitude). In the case of a periodic input, low temporal reliability would imply low phase locking and therefore the effect of the feedback would be to decrease the VS. Some cells in auditory cortex exhibit a similar behavior showing modulation of their rate up to stimulation frequencies of 300 Hz with almost no phase locking (Lu et al. 2001). Understanding the impact of network feedback on the ability of neurons to follow high frequency stimulation requires a separate study. This study should elucidate the basic mechanisms by which periodic information is transformed into asynchronous firing rate in both somatosensory and auditory cortical circuits.

4.4 Features not included in the model and future work

In this study we have focused our attention on the modeling of the thalamic response to different stimuli and on TC depression. These are important aspects to understand how the input currents coming into the barrel represent the temporal structure of the stimulus, but investigating the effect of the cortical network in shaping these inputs will be just as important or more. Thus, the present study must be viewed as the first step towards a more complete recurrent network model of the barrel, which should consider in particular both feed-forward and intra-cortical inhibition (Simons 1978; Swadlow 1989; Beierlein et al. 2003; Pinto et al. 2003). Including the cortico-thalamic feedback that VPM receives from cortex through inhibitory reticular neurons could also be important (Golomb et al. 2006). Another simplification taken here was to consider only steady state responses which can be easily compared with experiments but whose relevance when the rat is encoding a natural environment is questionable. Thus, analysis of the transient response is a necessary element to include in future work. Also not studied here, is the resonant amplification of the whisker amplitude at very high frequencies (Neimark et al. 2003). This feature could be included in the model by introducing a resonant dependence in the whisker motion amplitude, i.e. $A = A(f)$. Future work could address more fundamental questions related with the rat behavior, namely: What is the cortical response in the more realistic situation in which, while whisking at low frequencies (4–12 Hz), a vibrissa contacts a texture inducing resonant vibrations?; in this context, would a resonant

motion of the vibrissa (Andermann et al. 2004) give rise to a cortical response encoding the texture more optimally? what is the role played here by STD and velocity encoding?

Acknowledgements The research presented in this manuscript was supported by a grant from the Spanish Ministry of Education and Science (FIS 2006-09294). JR was also funded by a Postdoctoral Fellowship from the same institution. We thank Miguel Maraval and Alfonso Renart for critical reading of the manuscript.

Appendix 1

Values of the parameters

We take the synaptic parameters from *in vitro* and *in vivo* studies. In agreement with *in vitro* data obtained by Gil et al. (1999) we take as mean quantal EPSP size is $J/C_m \simeq 0.35$ mV with a coefficient of variation $\Delta \simeq 0.25$; mean number of release sites $M = 7$; release probability $U = 0.8$. In the absence of any spontaneous activity in the thalamus these values produce a mean EPSP amplitude $\langle PSP \rangle = MUJ/C_m = 1.96$ mV. Experiments in anesthetized and sedated rats have recently reported smaller mean amplitudes which depend on the animal state: for anesthetized animals mean = 1.94 mV (median 1.3 mV) whereas for sedated animals the mean = 0.49 mV (median 0.24 mV; Bruno and Sakmann 2006). These variation was accompanied with a difference in the spontaneous thalamic rate ($\nu_0 = 1.0$ Hz for anesthetized and 5.4 Hz for sedated (Bruno and Sakmann 2006)) suggesting that TC synapses are continuously depressed *in vivo* (Castro-Alamancos 2002; Bruno and Sakmann 2006). This continuous depression is expected to be larger in awake animals were spontaneous thalamic firing is even higher (~ 10 Hz; Fanselow and Nicolelis 1999; Swadlow and Gusev 2001). Finally, a different study in anesthetized rats has shown that the depressed TC EPSP amplitude recovers to rest values exponentially with a time constant $\tau_v \sim 5$ s (Chung et al. 2002). Had we used this value, which is almost two orders of magnitude larger than that measured in *in vitro* recordings of TC synapses in the visual system (Stratford et al. 1996), and spontaneous thalamic rates like those found *in vivo* (~ 5 – 10 Hz), we would have obtained an average TC EPSP lower than 0.05 mV. We therefore set $\tau_v = 300$ ms to reproduce average TC EPSP like those found in (Bruno and Sakmann 2006) when the spontaneous thalamic rate was 5 Hz.

We consider $N = 85$ thalamic neurons impinging onto the single target barrel cell based on an estimate of 200 cells per barreloid (Land et al. 1995; Varga et al. 2002) and a TC convergence ratio of 0.43 (Bruno and Sakmann 2006). Other parameters of the cortical cell model are: $\tau_m = 1 - 10$ ms, $\theta = 10-17$ mV, $H = 6-10$ mV, $\tau_{\text{ref}} = 2$ ms, $C_m = 100$ pF and $E_L = 0$. Background parameters: $M_E = 3$, $M_I = 6$, $J_E/C_m = 0.2$ mV, $J_I/C_m = -0.4$ mV, $U_E = U_I = 0.4$, $\nu_E = 5 \text{ ms}^{-1}$, $\nu_I = 1 \text{ ms}^{-1}$. The excitatory background rate being five times larger than the inhibitory background rate, reflects the approximate ratio of one inhibitory cell every five excitatory cells found in the cortex.

Appendix 2

The temporal contrast

The temporal contrast is defined as (Pinto et al. 2000):

$$\text{Temporal Contrast} = \frac{40\% \text{ of spikes per deflection}}{\text{time to produce 40\%}} \quad (14)$$

It measures in spiking rate units the mean firing rate of the early part of the response. Parameterizing the thalamic CPSTH with a Gamma function given by:

$$G(t) = \frac{C}{\Sigma} t e^{-t/\Sigma+1} \quad (15)$$

the temporal contrast can be evaluated easily: The numerator equals $0.4 e C \Sigma$, while the denominator is obtained by solving the equation:

$$\int_0^t G(z) dz = 0.4 e C \Sigma \quad (16)$$

which performing the integral becomes

$$\frac{t}{\Sigma} + \ln(1 - 0.4) = \ln\left(\frac{t}{\Sigma} + 1\right), \quad (17)$$

which yields to $t = 1.37 \Sigma$, giving finally:

$$\text{Temporal Contrast} = \frac{0.4 e C \Sigma}{1.37 \Sigma} \simeq 0.8 C \quad (18)$$

that is, it is simply proportional to the Gamma amplitude. Now, modeling the temporal contrast dependence on the velocity obtained by Pinto et al. (2000) using this Gamma parameterization implies that as the stimulus velocity increases the VPM response has to vary (1) increasing its amplitude C and (2) decreasing Σ so that the product $C\Sigma$ remains fixed. Doing so, the temporal contrast depends on the velocity while the spike count is independent of it.

References

- Abbott, L. F., Varela, J. A., Sen, K., & Nelson, S. B. (1997). Synaptic depression and cortical gain control. *Science*, *275*, 179–80.
- Ahissar, E., Sosnik, R., & Haidarliu, S. (2000). Transformation from temporal to rate coding in somatosensory thalamocortical system. *Nature*, *406*, 302–306.
- Andermann, M. L., Ritt, J., Neimark, M. A., & Moore, C. I. (2004). Neural correlates of vibrissa resonance; band-pass and somatotopic representation of high-frequency stimuli. *Neuron*, *42*(3), 451–63.
- Arabzadeh, E., Petersen, R. S., & Diamond, M. E. (2003). Encoding of whisker vibration by rat barrel cortex neurons: Implications for texture discrimination. *Journal of Neuroscience*, *23*(27), 9146–9154.
- Bazhenov, M., Rulkov, N. F., Fellous, J.-M., & Timofeev, I. (2005). Role of network dynamics in shaping spike timing reliability. *Physical Review E*, *72*, 041903.
- Beierlein, M., Gibson, J. R., & Connors, B. W. (2003). Two dynamically distinct inhibitory networks in layer 4 of the neocortex. *Journal of Neurophysiology*, *90*(5), 2987–3000.
- Borg-Graham, L., Monier, C., & Fregnac, Y. (1998). Visual input evokes transient and strong shunting inhibition in visual cortical neurons. *Nature*, *393*, 369–373.
- Brunel, N., Chance, F. S., Fourcaud, N., & Abbott, L. F. (2001). Effects of synaptic noise and filtering on the frequency response of spiking neurons. *Physical Review Letters*, *86*(10), 2186–2189.
- Bruno, R. M., & Sakmann, B. (2006). Cortex is driven by weak but synchronously active thalamocortical synapses. *Nature*, *312*, 1622–1627.
- Carandini, M., Heeger, D. J., & Senn, W. (2001). A synaptic explanation of suppression in visual cortex. *Journal of Neuroscience*, *22*, 10053–10065.
- Carvell, G., & Simons, D. (1990). Biometric analyses of vibrissal tactile discrimination in the rat. *Journal of Neuroscience*, *10*(8), 2638–2648.
- Castro-Alamancos, M. A. (1997). Short term plasticity in the thalamocortical pathways: Cellular mechanisms and functional roles. *Reviews in the Neurosciences*, *20*, 95–116.
- Castro-Alamancos, M. A. (2002). Different temporal processing of sensory inputs in the rat thalamus during quiescent and information processing states *in vivo*. *Journal of Physiology (Lond)*, *539*(2), 567–578.
- Castro-Alamancos, M. A., & Oldford, E. (2002). Cortical sensory suppression during arousal is due to the activity-dependent depression of thalamocortical synapses. *Journal of Physiology (Lond)*, *541*, 319–331.
- Chance, F. S., Abbott, L., & Reyes, A. D. (2002). Gain modulation from background synaptic input. *Neuron*, *35*, 773–782.
- Chance, F. S., Nelson, S. B., & Abbott, L. F. (1998). Synaptic depression and the temporal response characteristics of v1 cells. *Journal of Neuroscience*, *12*, 4785–4799.
- Chung, S., Li, X., & Nelson, S. B. (2002). Short-term depression at thalamocortical synapses contributes to rapid adaptation of cortical sensory responses *in vivo*. *Neuron*, *34*, 437–446.
- de la Rocha, J., Nevado, A., & Parga, N. (2002). Information transmission by stochastic synapses with short-term depression: Neural coding and optimization. *Neucomputing*, *44–46*, 85–90.
- de la Rocha, J., & Parga, N. (2005). Short-term synaptic depression causes a non-monotonic response to correlated stimuli. *Journal of Neuroscience*, *25*(37), 8416–8431.

- Deschenes, M., Timofeeva, E., & Lavalley, P. (2003). The relay of high-frequency sensory signals in the whisker-to-barreloid pathway. *Journal of Neuroscience*, *23*(17), 6778–6787.
- Eggermont, J. J. (1999). The magnitude and phase of temporal modulation transfer functions in cat auditory cortex. *Journal of Neuroscience*, *19*(7), 2780–2788.
- Fanselow, E. E., & Nicolelis, M. A. L. (1999). Behavioral modulation of tactile responses in the rat somatosensory system. *Journal of Neuroscience*, *19*(17), 7603–7616.
- Fleiderovich, I. A., Binshtok, A. M., & Gutnick, M. J. (1998). Functionally distinct NMDA receptors mediate horizontal connectivity within layer 4 of mouse barrel cortex. *Neuron*, *21*(5), 1055–1065.
- Garabedian, C. E., Jones, S. R., Merzenich, M. M., Dale, A., & Moore, C. I. (2003). Band-pass response properties of rat si neurons. *Journal of Neurophysiology*, *90*, 1379–1391.
- Gerstner, W. (2000). Population dynamics of spiking neurons: Fast transients, asynchronous states, and locking. *Neural Computation*, *12*(1), 43–89.
- Gerstner, W., & Kistler, W. (2002). *Spiking neuron models: Single neuron, populations, plasticity*. Cambridge University Press.
- Gil, Z., Connors, B. W., & Amitai, Y. (1999). Efficacy of thalamocortical and intracortical synaptic connections: Quanta, innervation, and reliability. *Neuron*, *23*, 385–397.
- Goldberg, J., & Brown, P. (1969). Response of binaural neurons of dog superior olivary complex to dichotic tonal stimuli: Some physiological mechanisms of sound localization. *Journal of Neurophysiology*, *32*, 613–636.
- Golomb, D., Ahissar, E., & Kleinfeld, D. (2006). Coding of stimulus frequency by latency in thalamic networks through the interplay of GABAB-mediated feedback and stimulus shape. *Journal of Neurophysiology*, *95*(3), 1735–1750.
- Hartings, J. A., & Simons, D. J. (1998). Thalamic relay of afferent responses to 1- to 12-Hz whisker stimulation in the rat. *Journal of Neurophysiology*, *80*(2), 1016–1019.
- Hartings, J. A., Temereanca, S., & Simons, D. J. (2003). Processing of periodic whisker deflections by neurons in the ventroposterior medial and thalamic reticular nuclei. *Journal of Neurophysiology*, *90*(5), 3087–3094.
- Hirsch, J. A., Alonso, J.-M., Reid, R. C., & Martinez, L. M. (1998). Synaptic integration in striate cortical simple cells. *Journal of Neuroscience*, *18*, 9517–9528.
- Hutcheon, B., & Yarom, Y. (2000). Resonance, oscillations and the intrinsic frequency preferences of neurons. *Trends in Neuroscience*, *23*(5), 216–222.
- Khatri, V., Hartings, J. A., & Simons, D. J. (2004). Adaptation in thalamic barreloid and cortical barrel neurons to periodic whisker deflections varying in frequency and velocity. *Journal of Neurophysiology*, *92*(6), 3244–3254.
- Koch, C. (1999). *Biophysics of computation: Information processing in single neurons*. Oxford University Press.
- Land, P. W., Buffer, S. A., & Yaskosky, J. D. (1995). Barreloids in adult rat thalamus: Three-dimensional architecture and relationship to somatosensory cortical barrels. *The Journal of Comparative Neurology*, *355*(4), 573–588.
- Lichtenstein, S., Carvell, G., & Simons, D. (1990). Responses of rat trigeminal ganglion neurons to movements of vibrissae in different directions. *Somatosensory & Motor Research*, *7*, 47–65.
- Lin, K. K., Shea-Brown, E., & Young, L.-S. (2007). Reliability of coupled oscillators I: Two-oscillator systems. Submitted to *Journal of Nonlinear Science*. Available online: <http://arxiv.org/abs/0708.3061>.
- Lu, T., Liang, L., & Wang, X. (2001). Temporal and rate representations of time-varying signals in the auditory cortex of awake primates. *Nature Neuroscience*, *4*, 1131–1138.
- Magleby, K. L. (1987). Short-term changes in synaptic efficacy. In G. Edelman, W. Gall, & W. Cowan (Eds.), *Synaptic function* (pp. 21–56). New York: Wiley.
- Matveev, V., & Wang, X.-J. (2000). Implications of all-or-none synaptic transmission and short-term depression beyond vesicle depletion: A computational study. *Journal of Neuroscience*, *20*, 1575–1588.
- Moore, C. I. (2004). Frequency-dependent processing in the vibrissa sensory system. *Journal of Neurophysiology*, *91*, 2390–2399.
- Neimark, M. A., Andermann, M. L., Hopfield, J. J., & Moore, C. I. (2003). Vibrissa resonance as a transduction mechanism for tactile encoding. *Journal of Neuroscience*, *23*(16), 6499–6509.
- Pinto, D. J., Brumberg, J. C., & Simons, D. J. (2000). Circuit dynamics and coding strategies in rodent somatosensory cortex. *Journal of Neurophysiology*, *83*(3), 1158–1166.
- Pinto, D. J., Hartings, J. A., Brumberg, J. C., & Simons, D. J. (2003). Cortical damping: Analysis of thalamocortical response transformations in rodent barrel cortex. *Cerebral Cortex*, *13*, 33–44.
- Ricciardi, L. M. (1977). *Diffusion processes and related topics in biology*. Berlin: Springer.
- Rieke, F., Warland, D., de Ruyter van Steveninck, R. R., & Bialek, W. (1996). *Spikes: Exploring the neural code*. Cambridge, MA: MIT Press.
- Shoykhet, M., Doherty, D., & Simons, D. (2000). Coding of deflection velocity and amplitude by whisker primary afferent neurons: Implications for higher level processing. *Somatosensory & Motor Research*, *17*, 171–18.
- Simons, D. J. (1978). Response properties of vibrissa units in rat si somatosensory neocortex. *Journal of Neurophysiology*, *41*, 798–820.
- Sosnik, R., Haidarliu, S., & Ahissar, E. (2001). Temporal frequency of whisker movement. I. Representations in brain stem and thalamus. *Journal of Neurophysiology*, *86*(1), 339–353.
- Stratford, K., Tarczy-Hornoch, K., Martin, K., Bannister, N., & Jack, J. (1996). Excitatory synaptic inputs to spiny stellate cells in cat visual cortex. *Nature*, *382*, 258–261.
- Svirskis, G., & Rinzel, J. (2003). Influence of subthreshold nonlinearities on signal-to-noise ratio and timing precision for small signals in neurons: Minimal model analysis. *Network: Computation in Neural Systems*, *14*(1), 137–150.
- Swadlow, H. (1989). Efferent neurons and suspected interneurons in s1 vibrissa cortex of the awake rabbit: Evidence from cross-correlation, microstimulation, and latencies to peripheral sensory stimulation. *Journal of Physiology*, *62*, 288–308.
- Swadlow, H. A., & Gusev, A. G. (2001). The impact of ‘bursting’ thalamic impulses at a neocortical synapse. *Nature Neuroscience*, *4*(4), 401–408.
- Tsodyks, M. V., & Markram, H. (1997). The neural code between neocortical pyramidal neurons depends on neurotransmitter release probability. *Proceedings of the National Academy of Sciences of the United States of America*, *94*, 719–723.
- Varga, C., Sik, A., Lavalley, P., & Deschenes, M. (2002). Dendroarchitecture of relay cells in thalamic barreloids:

- A substrate for cross-whisker modulation. *Journal of Neuroscience*, 22(14), 6186–6194.
- Vere-Jones, D. (1966). Simple stochastic models for the release of quanta of transmitter from a nerve terminal. *Australian Journal of Statistics*, 8, 53–63.
- Wang, X.-J. (1999). Fast burst firing and short-term synaptic plasticity: A model of neocortical chattering neurons. *Neuroscience*, 89(2), 347–362.
- Welker, W. (1964). Analysis of sniffing of the albino rat. *Behavior*, 12, 223–244.
- Welker, W. I., Johnson Jr., J. I., & Pubols Jr., B. H. (1964). Some morphological and physiological characteristics of the somatic sensory system in raccoons. *American Zoologist*, 136, 75–94.
- Zucker, R. S., & Regehr, W. G. (2002). Short-term synaptic plasticity. *Annual Review of Physiology*, 64, 355–405.